Numerical Modeling of Millimeter Wave Transmission Lines

Georg Michel

December 17, 2010

Abstract

The transmission of high-power millimeter waves for electron cyclotron resonace heating of plasmas is a well developed field which has reached a mature level over the years [1]. The design goals are low transmission losses, high mode purity and arbitrary polarization adjustment with low cross polarization. Quasi-optical and waveguide techniques are at hand for the design of transmission lines which in most cases are a combination of both approaches. This article discusses the efficient numerical processing of paraxial beams and fields in oversized corrugated waveguides including polarization, and how these methods can be used for the analysis, synthesis and modeling of the RF fields from the gyrotron cavity to the plasma.

1 Introduction

In transmission lines there is usually only a unidirectional interaction between optical elements, i.e. there are no resonating or backscattering structures. In most cases it is therefore not necessary to make use of selfconsistent calculations like the method of moments or Fox-Li iterations, which basically correspond to a Born approximation of high order. The main goal in transmission line calculations is simply to speed up the diffraction integral from one aperture to the next, either in free space or in a waveguide. Hence, with n optical elements, a Born approximation of n-th order is sufficient for a correct calculation of the field in the whole transmission line.

Paraxial beams in millimeter wave transmission lines are commonly represented as Gauss-Hermite or Gauss-Laguerre modes. They are called "modes" because they where first observed as eigenmodes of Laser resonators. In transmission systems, however, they are actually used as a set of orthonormal basis functions to represent a wave beam which ideally consists only of the fundamental "mode". This is a simple and powerful approach for the handling of such systems due to the virtually finite support of these functions and the fact that only two parameters change along the optical axis, namely the beam radius and wavefront curvature. These basis functions, however, are inexpedient when it comes to the numerical processing of realistic arbitrary field profiles as there is an infinite number of basis functions the contribution of which has to be determined with a two-dimensional integral. Therefore a common method is

to substitute the the actual beam with the best fit of a fundamental Gaussian beam.

Another possible set of basis functions which at first glance seems to be inappropriate are plane waves. They have an infinite support, and there are as many changing parameters along the optical axis as there are plane waves, which may be millions. Nevertheless, there is one advantage: The fast Fourier transform (FFT) can be used to decompose and propagate a numerically given field efficiently. In the following sections simple formulas will be introduced for the efficient calculation of the propagation of real field profiles in transmission lines consisting of mirrors and corrugated waveguides. This makes the implementation of a number of iterative algorithms for the analysis and synthesis of components possible which will be briefly summarized in section 4.

2 Field Propagation in Free Space and Corrugated Waveguides

2.1 Free Space

The calculation of the electromagnetic field is greatly simplified for our purposes by the introduction of the electric vector potential $\mathbf{F}$. Equivalently, we could use the magnetic Hertzian potential $\mathbf{\Pi}_h$ with the relation $j\omega\mathbf{\Pi}_h = c^2\mathbf{F}$. With the Lorentz gauge we obtain

$$\mathbf{E} = -\nabla \times \mathbf{F}/\varepsilon_0 \quad (1)$$

$$\mathbf{H} = -j\omega\mathbf{F} - jc^2\nabla(\nabla \cdot \mathbf{F})/\omega. \quad (2)$$

Throughout the paper a harmonic time dependency of $e^{+j\omega t}$ with $j^2 = -1$ is assumed. Bold symbols are vectors and bold symbols with a bar are dyadic tensors.

Although the field extends over three dimensions, it is usually only calculated on planes, called apertures, which are positioned arbitrarily in the three-dimensional space. This eliminates, for wave beams, the redundancy of a three-dimensional representation and makes the numerical effort feasible. We can reduce the problem to the solution of the scalar wave equation by using the ansatz

$$\mathbf{F}(x, y, 0) = u(x, y)\mathbf{F}_0 \quad (3)$$

where u is a scalar function of the aperture coordinates, and $\mathbf{F}_0$ is a constant three-dimensional complex vector. This scalar ansatz leads to considerable savings in CPU time and memory but still provides a fully qualified solution of the Maxwell equations. $\mathbf{F}_0$ usually is perpendicular to the beam axis, it can thus represent a paraxial beam through the aperture with an arbitrary and possibly elliptical polarization. The beam axis is not necessarily perpendicular to the aperture. An ansatz with a constant $\mathbf{E}_0$ or $\mathbf{H}_0$ would not be correct as the ratio of their components can not be constant. It would nonetheless be possible to solve e.g for H_y only while requiring $E_y = 0$. The other field components can then be derived from H_y via the Maxwell equations. Nevertheless, the use of the electric vector potential $\mathbf{F}$ is more convenient for our purposes.

The kernel of the diffraction integral between two parallel apertures depends only on the difference of their local coordinates, and therefore represents a two-

dimensional convolution. Here we can easily make use of the FFT by translating the numerically expensive convolution in the location domain into a simpler multiplication in the wave number domain. This is known as the plane wave decomposition. For non-parallel apertures, the operation in the spectral domain is no longer a mere multiplication:

$$\mathcal{F}u_t(k_x, k_y) = \frac{1}{k_z}\mathcal{F}u_s([\bar{\mathbf{S}}^T\bar{\mathbf{T}}\mathbf{k}]_x, [\bar{\mathbf{S}}^T\bar{\mathbf{T}}\mathbf{k}]_y)\beta([\bar{\mathbf{S}}^T\bar{\mathbf{T}}\mathbf{k}]_z)e^{-j[\bar{\mathbf{T}}\mathbf{k}]_z d} \tag{4}$$

Here, $\mathcal{F}u_{t,s}$ are the Fourier transforms of u in the target and the source aperture. The Fourier transform is usually defined for the spatial frequency $\mathbf{f}$ as

$$\mathcal{F}u(f_x, f_y) = \iint_{-\infty}^{\infty} u(x, y)e^{-j2\pi(f_x x + f_y y)}\, dx\, dy. \tag{5}$$

Nevertheless we will use the more intuitive wave number $\mathbf{k} = -2\pi\mathbf{f}$ with $\mathbf{k} = (k_x, k_y, \sqrt{k_0^2 - k_x^2 - k_y^2})^T$, β is the ramp function and d is the distance between the centers of the apertures. $\bar{\mathbf{T}}$ and $\bar{\mathbf{S}}$ are the rotation tensors which transform the local coordinates of the target and source apertures into a canonical coordinate system. Hence, their columns are the base vectors of the local systems expressed in terms of the canonical system and they are orthonormal, i.e. $\bar{\mathbf{D}}^{-1} = \bar{\mathbf{D}}^T$. Both aperture centers lie on the z-axis of the canonical system. The optical elements in a real application with mirrors, vacuum windows and waveguides are usually not on the z-axis of a canonical system. Instead, there is a conveniently chosen global coordinate system in which the locations of the target and source apertures are $\mathbf{t}$ and $\mathbf{s}$. Now a third tensor $\bar{\mathbf{R}}$ is chosen to render $\bar{\mathbf{R}}(\mathbf{t} - \mathbf{s}) = (0, 0, d)^T$. This tensor is used to obtain

$$\begin{aligned} \bar{\mathbf{T}} &= \bar{\mathbf{R}}\bar{\mathbf{T}}' \\ \bar{\mathbf{S}} &= \bar{\mathbf{R}}\bar{\mathbf{S}}' \end{aligned} \tag{6}$$

where the columns of $\bar{\mathbf{T}}'$ and $\bar{\mathbf{S}}'$ represent the base vectors of the local coordinate systems in terms of the global system. The easiest way to calculate $\bar{\mathbf{R}}$ is to take $(\mathbf{t} - \mathbf{s})/d$ as the third column of $\bar{\mathbf{R}}^{-1}$. The unit length vector product with another freely chosen vector provides the first column. Finally, the second column is the vector product of the third and first column. Now $\bar{\mathbf{R}}^{-1}$ can be inverted (i.e. transposed because of the orthonormality). For a derivation of (4) the reader is referred to [2].

Equation (4) is a generalization of the plane wave decomposition. As the arguments of $\mathcal{F}u_t$ and $\mathcal{F}u_s$ are generally not identical, this operation is not a 2D convolution anymore (i.e. an interpolation is necessary in a computer code). However, if both apertures have the same orientation (but are not necessarily perpendicular to the optical axis), $\bar{\mathbf{S}}^T\bar{\mathbf{T}}$ results in the unity tensor and we again have a convolution. If both apertures are perpendicular to the optical axis, (4) is reduced to the well kown formula for the plane wave decomposition. This formula can be used for the backward transform of a given field by simply taking a negative distance to the source aperture. Equation (4) has the same property when u_t, u_s, $\bar{\mathbf{T}}$ and $\bar{\mathbf{S}}$ are interchanged accordingly while keeping d positive. The only condition that must be fulfilled is that the scalar product between both local z-axes is kept positive. If the target aperture is positioned in the

positive-z-half-space of the source aperture, we have a forward transform. If it is in its negative half-space, we have a backward transform (see [2] for details). Therefore similar to the plane wave decomposition there is no difference between the forward and the backward propagator.

An approximate solution to the tilted-aperture problem is the use of virtual apertures that are perpendicular to the optical axis with a scaling of the tilted transverse coordinate in accordance with the cosine of the tilt angle [3]. In addition, the longitudinal phase shift along this coordinate has to be imposed. However, this method neglects the beam diffraction over the longitudinal extent of the tilted aperture. For a diverging or converging fundamental Gaussian beam for example, the field takes the shape of an ellipse with this method, whereas with (4) it looks like a conic section due to the beam divergence.

When using this propagator, the laws of the multi-dimensional Fourier transform have to be kept in mind (see e.g. [4]). The discretization in the wave number domain leads to a periodification in the location domain. This means that the required aperture size must be achieved with a small enough sampling distance in the wavenumber domain. The sampling distance in the location domain, on the other hand, must be small enough to fulfill the Nyquist theorem. Both restrictions together determine the total number of sampling points. However, the Nyquist theorem must be fulfilled only for the *transverse* wavenumber which is much smaller than k_0 (this is actually the definition of a paraxial beam). This fact is helpful for large d which let the phase term in (4) oscillate quickly and require thus a small sampling distance. As the amplitude distribution in the wave number domain does not change, it is now possible to concentrate the calculation area around the "mass center" of the beam in the wave number domain in order to decrease the sampling distance. This enlarges the aperture in the location domain without increasing the required number of sampling points. The same can be done e.g. for a focus in the location domain which would require a smaller sampling distance there. By accounting for these principles it is possible to handle even large setups with a feasible numerical effort [5].

2.2 Corrugated Waveguides

The plane wave decomposition in the above section uses a finite number of basis functions or "modes" to represent the field in free space. This is equivalent to considering the free space as an extremely overmoded waveguide with a very dense mode spectrum in which the walls are at a sufficient distance from the paraxial beam. If they come too close we can observe "reflections" from these virtual waveguide walls, which is nothing other than aliasing from the above mentioned periodification.

Whereas this is a limiting factor for the free space model, we can harness this effect for the propagation in oversized corrugated waveguides. The corrugation on their inner wall basically leads to an anisotropic surface impedance that creates so-called artificially soft boundary conditions [6]. This term is borrowed from acoustics and stresses the polarisation-independent reflection coefficient for a low-grazing-angle reflection. Transverse corrugations represent soft boundary conditions ($E_\perp = E_\parallel = 0$), whereas longitudinal corrugations lead to hard boundary conditions with surface waves and $\partial E_\perp/\partial n = \partial E_\parallel/\partial n = 0$. The latter have higher losses, which is the reason why they are rarely used in high-power applications.

Because of the low Brillouin angle of modes far from cutoff, the assumption of ideally soft boundary conditions is justified for strongly overmoded corrugated waveguides [6], [7]. A rigorous treatment of modes without this restriction can be found in [8].

TE modes in a smooth waveguide can be derived by solving the scalar Helmholtz equation for an $\mathbf{F}$ that has only a longtitudinal component. Due to the assumption of soft boundary conditions, we can now make use of (3) where $\mathbf{F}$ has only a transverse component. Different to the Neumann boundary conditions for the TE modes, we now have to choose Dirichlet (soft) boundary conditions for this ansatz. This gives a set of transverse modes in the corrugated waveguides that has a high coupling to the Gauss-Hermite basis functions for rectangular waveguides and to the Gauss-Laguerre functions for circular waveguides. It is therefore justified to consider these modes as "captured" waist fields of Gauss-Hermite/Laguerre beams.

In order to use the plane wave decomposition in a rectangular corrugated waveguide we just propagate the modes which fulfill the boundary conditions according to their transverse wavenumber. This is simple and trivial. However, rectangular corrugated waveguides are only used if imaging characteristics are required, e.g. for remote steering antennas [9] or beam splitters [10].

For the commonly used circular corrugated waveguides the Helmholtz equation must be solved in cylindrical coordinates. This leads to the well known set of orthonormal cylindrical modes

$$u(r,\varphi) = \sum_{m=-M}^{M} \sum_{n=1}^{N(M)} A_{mn} u_{mn}(r,\varphi) \tag{7}$$

$$u_{mn}(r,\varphi) = \frac{J_{|m|}\left(\frac{\chi_{|m|n}}{a} r\right) e^{jm\varphi}}{a\sqrt{\pi}|J_{|m|+1}(\chi_{|m|n})|} \tag{8}$$

where a is the waveguide radius, $\chi_{|m|n}$ is the n-th root of $J_{|m|}$ and A_{mn} are the mode amplitudes to be calculated and to be multiplied by the phasor $e^{-jz\sqrt{k_0^2-\chi_{|m|n}^2/a^2}}$. Now a fast cylindrical wave decomposition is needed instead of the plane wave decomposition. A straight forward approach would obtain the A_{mn} by calculating the scalar product of the field with the corresponding basis functions. For a wavegide with thousands of propagating modes this would be numerically expensive. However, it is possible to obtain the A_{mn} efficiently even without an evaluation of the Bessel functions. First, the spectrum has to be represented in polar coordinates by interpolating $U(k_r,\phi) = (\mathcal{F}u)(k_r\cos\phi, k_r\sin\phi)$ where $\mathcal{F}u$ is calculated via the FFT. Now the spectrum is again decomposed into circular harmonics with a series of one-dimensional FFTs:

$$U_m(k_r) = \frac{1}{2\pi}\int_0^{2\pi} U(k_r,\phi)e^{-jm\phi}d\phi. \tag{9}$$

Note that the number of harmonics increases with k_r, as the circular sampling also has to fulfill the Nyquist theorem. When the unknown $U_m(k_r)$ are found we can obtain the mode amplitudes

$$A_{mn} = \frac{j^m U_m(\chi_{|m|n}/a)}{2a\pi^{3/2}|J_{|m|+1}(\chi_{|m|n})|}. \tag{10}$$

The $J_{|m|+1}(\chi_{|m|n})$ can be taken from a table, see [2] for a derivation of (10).

The remaining problem is the recomposition of the propagated modes. An unbound normal mode (7) is a Dirac ring in the wavenumber domain which is easy to represent numerically. But the field in a waveguide is limited by the waveguide walls which blurs the δ-ring[1]. The calculation of such a blurred ring would be a convolution of the δ-ring with the spectrum of the waveguide cross section, a so-called Sombrero-function. This is certainly too expensive, as it has to be done for every mode. For this reason the recomposition is approached in a different way. First, the circular harmonics have to be calculated for every sampled value of r:

$$u_m(r) = \sum_n \frac{A_{mn}}{a\sqrt{\pi}|J_{|m|+1}(\chi_{|m|n})} J_{|m|}\left(\frac{\chi_{|m|n}}{a} r\right) \tag{11}$$

Then (7) can be calculated by a number of one-dimensional FFTs:

$$u(r,\varphi) = \sum_{m=-M}^{M} u_m(r) e^{jm\varphi}. \tag{12}$$

Finally $u(x,y)$ is obtained with another interpolation of $u(r,\varphi)$. Generally, we could also use this technique for paraxial beams in free space, similar to the plane wave decomposition. However, this would be inappropriate as (4) is faster and simpler. In a transmission line simulation, the field can now easily be handed over from the free-space propagator to the waveguide propagator and vice versa, in accordance with the transmission path.

The decomposition and propagation of cylindrical modes can be applied to straight waveguides, where the computational effort does not depend on the waveguide length. However, if there are wall perturbations or curvature, this method is no longer applicable. The classical solution to this problem would be the coupled mode technique [8],[11]. But we can also successively calculate the diffraction integral from the waveguide wall to itself. The price of this approach is that the diffraction integral has to be solved as often as the Brillouin length of the highest order mode fits into the waveguide length (i.e. a Born approximation of n-th order is calculated). The Brillouin length is the longitudinal distance between two bounces of a ray in the geometrical optics model of a cylindrical mode.

It can easily be verified that the kernel of the diffraction integral from a circular waveguide wall to itself is location-independent, i.e. it depends only on $\Delta\varphi$ and Δz. This corresponds to a linear time-independent system in signal theory, and hence we can carry out the convolution in the spectral domain by means of the FFT. The wall discontinuities can then act as a phase corrector if all modes have a similar $k_\perp$. Another approach which describes the same physics is the utilization of the fact that cylindrical modes are longitudinally and azimuthally harmonic. This can be used for a fast mode (de)composition via a 2D FFT over the waveguide wall. This approach is decribed in [12],[13].

[1] A sharp δ-ring would require an infinitesimally small sampling distance anyway.

3 Representation of the Field Quantities

3.1 Integration with Full-Wave Codes

The starting point for the numerical model of a transmission line is the source field. In ECRH transmission lines it emanates from a helically cut waveguide with wall perturbations that is driven by a rotating high-order TE mode [11],[13]. The field which is radiated from the helical cut can be calculated with the coupled mode approach [11] or with the scalar diffraction integral [13]. Nevertheless, the most accurate results are achieved by the direct numerical solution of Maxwell's equations with a MoM code [14] where the complete geometry can be modeled and no approximations are made except from the discretization. However, the calculation of the complete transmission line up to the plasma with such a code is more or less unfeasible due to the very large structures compared to the wavelength.

The aforementioned scalar approach can handle the large structures efficiently, but it requires the field in a vector potential representation. Therefore an interface from the full-wave code to the scalar code is required. This involves the "inverse" problem of finding a vector potential that results in the numerically given field. Moreover, (3) must be able to represent this vector potential. This is the case when we can find an aperture where the **E**-field has a negligible z-component in its local coordinate system (TE waves). The aperture does not necessarily have to be perpendicular to the direction of propagation. In our case this happens to be in a plane perpendicular to the gyrotron axis and at a short distance above the quasi-elliptical mirror[2] where the field can be calculated with a commercial MoM code (e.g. [14]). In this plane **E** has a vanishing z-component. Because of (1) we can now define $\mathbf{F} = [0, 0, u(x, y)]^T$ in the local coordinate system.

The scalar function $u(x, y)$ can be found with a variational approach. We look for a best solution as per the definition of the vector potential by making the functional

$$I(u) = \iint \left(\left| -E_x - \frac{\partial u}{\partial y} \right|^2 + \left| E_y - \frac{\partial u}{\partial x} \right|^2 \right) dx\, dy \tag{13}$$

stationary. Here we can again make use of the FFT. When E_x, E_y and u are represented as a Fourier series, setting $\delta I = 0$ gives the Fourier coefficients c_{ik} of u in terms of the Fourier coefficients a_{ik} of E_x and b_{ik} of E_y:

$$c_{ik} = \frac{ib_{ik} - ka_{ik}}{j(i^2 + k^2)}. \tag{14}$$

With a Fourier backtransform we obtain the field $\mathbf{F} = u(x, y)\mathbf{e}_z$ according to (3). See [15] for an example.

After the traversal through all the mirrors, waveguides and polarizers, the result can be converted back to the field quantities **E** and **H** e.g. to integrate with a full-wave plasma physics code. This rather trivial conversion will be discussed in section 3.4.

[2] ... or the last deep mirror if there are several.

3.2 Beam Reflection on Mirrors and Polarizers

The remaining shallow mirrors inside and outside the gyrotron can be regarded as plane phase correctors that permit the field representation in plane apertures. They are considered as a thin lens that applies only a phase shift to the field distribution. This phase shift is the optical retardation caused by the shallow height modulation Δz of the surface:

$$u_{\mathrm{new}}(x,y) = u_{\mathrm{old}}(x,y) \cdot e^{j4\pi\Delta z \cos(\theta)/\lambda}. \tag{15}$$

Here, θ is the angle between the "mass center" of the paraxial beam in the wavenumber domain, and the z-axis of the aperture.

The height modulation of a mirror does not only introduce a phase shift, but generally also cross-polarization. However, as the mirror surface is shallow, the mirror can be considered as a plane surface for the alteration of $\mathbf{F}_0$ after the reflection. The ansatz (3) is based on this assumption. The electric field of a plane wave on the (at first plane) mirror surface is according to (1)

$$\mathbf{E}_0(\mathbf{r}) = \frac{-j}{\varepsilon_0} \begin{Bmatrix} 0 & k_z & -k_y \\ -k_z & 0 & k_x \\ k_y & -k_x & 0 \end{Bmatrix} \mathbf{F}_0 e^{-j\mathbf{k}\cdot\mathbf{r}}. \tag{16}$$

When we express the incident and the reflected dominating plane wave by (16) and impose $\mathbf{E}_{\parallel} = 0$ as for a perfect electric conductor we can find $\mathbf{F}_0$ and the wave vector of the reflected wave by a comparison of coefficients: $\mathbf{k}^r = (k_x^i, k_y^i, -k_z^i)^T$ and $\mathbf{F}_0^r = (F_{0x}^i, F_{0y}^i, -F_{0z}^i)^T$.

This is handled in a so-called "reflection" operation which turns a mirror surface into a source that previously was a target. This operation takes care of the mentioned constraint regarding the position of the target and source aperture in their local coordinate systems. A paraxial beam in an aperture originates from $z < 0$ and emanates into $z > 0$ in its local coordinate system according to section 2.1. In order to model a reflection on a shallow mirror, the beam is first propagated to its aperture via (4) where the local $\mathbf{F}_0$ is set by transforming the $\mathbf{F}_0$ of the source aperture into the global coordinate system, and from there into the local coodinate system of the target. This is achieved with the tensors $\bar{\mathbf{S}}'$ and $\bar{\mathbf{T}}'$ (6). Then the local coordinate system is rotated by 180° around its y-axis so that the local z axis (and hence the z-component of the beam axis) points into the opposite direction. Note that $u(x,y) := u(-x,y)$ has to be imposed too because the aperture field in the global coordinate sytem should not change due to this rotation. For the same reason we let $F_{0x} := -F_{0x}$ but not $F_{0z} := -F_{0z}$, as the direction reversal of F_{0z} is intended to fulfill the boundary conditions. Now we can apply (15) which completes the reflection operation for a shallow mirror.

For polarizers, the recalculation of $\mathbf{F}_0$ must be handled differently. Here we employ the Jones matrix formalism which is widely used in optics. In this approach the reflected electrical field is obtained by a multiplication of the incident field with the 3D Jones matrix [16]:

$$\mathbf{E}^r = \begin{Bmatrix} f & 0 & 0 \\ \frac{-fk_yk_x}{k_y^2+k_z^2} & \frac{-sk_z^2}{k_y^2+k_z^2} & \frac{-sk_yk_z}{k_y^2+k_z^2} \\ \frac{-fk_zk_x}{k_y^2+k_z^2} & \frac{sk_yk_z}{k_y^2+k_z^2} & \frac{sk_y^2}{k_y^2+k_z^2} \end{Bmatrix} \mathbf{E}^i \tag{17}$$

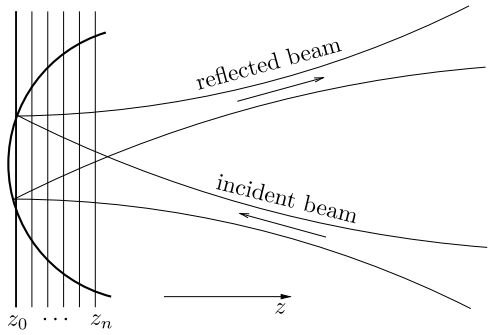

Figure 1: A Deep Mirror Modeled with Staggered Apertures

In this equation $\mathbf{k}$ stands for the dominant plane wave vector in the local coordinate system where k_z is always positive, before and after the rotation. The phasors s and f account for the slow and fast polarization ($\mathbf{E}$-field perpendicular or parallel to the grooves):

$$f = -e^{2jk_z d} \tag{18}$$

$$s = \frac{w\sqrt{k_y^2+k_z^2}\tan\left(d\sqrt{k_y^2+k_z^2}\right)+jpk_z}{w\sqrt{k_y^2+k_z^2}\tan\left(d\sqrt{k_y^2+k_z^2}\right)-jpk_z}\cdot f \tag{19}$$

These equations hold for rectangular grooves along the local x-axis with a groove width of w, a depth of d and a period of p. The reference plane $z = 0$ is at the bottom of the grooves. It can be easily verified that (17)-(19) results in the boundary conditions for a smooth surface when $d = 0$ and it yields the appropriate phase shift for perpendicular beams in fast and slow polarization for ideal grooves ($w = p$). Other than our model, most high-power polarizers have sinusoidal grooves. However, with a least squares fit to a full-wave calculation or a measurement it is possible to obtain an "effective" rectangular groove depth which shows the same characteristics as the sinusoidal grooves [16]. Therefore we can use this simple model in transmission calculations.

In order to obtain $\mathbf{F}_0^r$, $\mathbf{E}^i$ is first calculated via (16). Then $\mathbf{E}^r$ is obtained with (17). Unfortunately we cannot simply invert the matrix in (16) to calculate $\mathbf{F}_0^r$, as it is of rank 2. This is only natural because (1) is not bijective. We can overcome this problem by introducing a reasonable constraint on $\mathbf{F}_0^r$. By requiring $\mathbf{F}_0^r \cdot k_0^r = 0$ we force the beam to have no cross polarization in the outer regions, which is reasonable for our purposes. We therefore first transform $\mathbf{E}^r$ into a coordinate system where the dominant plane wave of the reflected beam $\mathbf{k}^r$ has only a z-component. This eliminates the third row and the tird column in (16). In this coordinate system E_z^r is negligible or zero as we have TEM waves. Due to the above constraint F_{0z}^r also vanishes in this coordinate system, which reduces (16) to two independent equations for F_{0x} and F_{0y}. The resulting $\mathbf{F}_0^r$ can now be transformed back to the local coordinate system of the aperture which completes the recalculation of $\mathbf{F}_0$ for a polarizer.

A mirror can not be modeled as a mere phase corrector if the amplitude distribution of the incident beam changes significantly over its longitudinal extent. In this case we can still model the reflection with a set of staggered phase

correctors at z_k as shown in Figure 1. In this scheme each aperture considers points with $z > z_k - \Delta z/2$ as belonging to the k-th aperture where Δz is the distance between the apertures. Except from $e^{-j\mathbf{k}_i \cdot \mathbf{r}}$, the field distribution should not change significantly over Δz. Now the reflected beam in aperture n can be calculated with the following scheme:

1. Initialize k to zero.
2. Calculate the phase-corrected reflected beam on the k-th aperture.
3. Replace the field for points not belonging to the k-th aperture with the field from the temporary aperture[3].
4. Place the temporary aperture at position $k+1$ and propagate the field to it.
5. If $k < n$: increment k and go back to step 2.

In the first run of this loop the error will be quite large, but it becomes smaller with every iteration until $k = n$ is reached. Now the reflected beam is available in the aperture at z_n. It should be mentioned again that (3) is not always suitable for deep mirrors because of the introduction of cross polarization on deep mirrors in general. Nevertheless, it is posible to use this method for the deep mirror(s) in front of the gyrotron launcher, as the direction of $\mathbf{F}_0$ relative to the surface does not change in this case. Due to the FFT, the computing time for this approach is $\mathcal{O}(N \log N)$ as compared to $\mathcal{O}(N^2)$ for the straight forward convolution. This speed advantage is of the same order as that of a fast multipole method. Nevertheless, the above scheme fits better in our framework, and it is less complex in its implementation. In the fast multipole approach, the approximation is in the series expansion of the Green function, whereas in our approach the thin lens approximation has to be taken into account. However, a concise comparison has not been done up to now.

3.3 Longitudinal Projection

During the analysis of a transmission line it is often helpful to see a longitudinal projection or "X-ray image" of a beam as depicted in Figure 1, e.g for the identification of side lobes. The field in an aperture contains the complete information about a beam, and can be used to produce such an image. Here we can apply the projection-slice theorem which is the basis of tomographic image reconstruction. It relates the one-dimensional Fourier transform of the projection

$$p(x) = \int_{-\infty}^{\infty} u(x, y)\, dy \tag{20}$$

to the two-dimensional spectrum of $u(x, y)$. The identity

$$\mathcal{F}_{x,y} u(k_x, 0) = \mathcal{F}_x p(k_x) \tag{21}$$

becomes evident by writing down the two-dimensional Fourier integral for $u(x, y)$ and setting $k_y = 0$. We can now calulate such a longitudinal projection efficiently by first placing an aperture so that its local x-z-plane is the desired

[3]Note that all points belong to the zero-th aperture where the temporary aperture is still undefined.

projection plane. Now we calculate $\mathcal{F}_x p(k_x)$ via (21). The actual projection in the x-z-plane is then obtained by a one-dimensional inverse FFT for each z:

$$p(x,z) = \mathcal{F}_x^{-1}\left(\mathcal{F}_x p(k_x,0) e^{-j\sqrt{k_0^2-k_x^2}z}\right). \tag{22}$$

We can easily see that this is a one-dimensional plane wave decomposition for $p(x)$.

3.4 Spill-Over and Screening

One of the most common tasks in the evaluation of a transmission line is the determination of the spill-over on a mirror or the screening due to the limited area of a vacuum window. The framework described here does not allow the proper modeling of edge diffraction effects but we can obtain the fraction of power that misses (or hits) a certain area on an aperture. In this way we can obtain the spill-over or screening losses for our purposes.

As $\mathbf{E}$ and $\mathbf{H}$ are proportional to $\mathbf{F}$ according to (1)-(3), we might be tempted to just calculate $|u(x,y)|^2$ and to find out the fraction that falls into the area of interest. But this is only a rough approximation that neglects the curvature of the wavefront. Especially in high-power applications where 1% of the total power can already have severe effects, we must include the contribution of the curvature. Therefore we have to calculate the longitudinal component of the Poynting vector

$$S_\parallel = \frac{1}{2}\Re\{(\mathbf{E}\times\mathbf{H}^*)\cdot\mathbf{e}_z\} \tag{23}$$

in order to obtain the power distribution. In fact there will be no imaginary part because we consider propagating waves only. First we have to obtain $\mathbf{E}$ and $\mathbf{H}$ which is also required if we want to interface with other codes (see section 3.1). Now it would be possible but not wise to use finite differences to calculate $\mathbf{E}$ and $\mathbf{H}$ from (1)-(3). As the field propagation is done in the spectral domain anyway, we can compute the derivative more efficiently by making use of $\mathcal{F}(\partial u/\partial[x,y,z]) = j2\pi f_{[x,y,z]}\mathcal{F}u = -jk_{[x,y,z]}\mathcal{F}u$. From (1)-(3) we finally obtain

$$\mathbf{E}(x,y) = \mathcal{F}^{-1}\frac{-j\mathcal{F}u(k_x,k_y)}{\varepsilon_0}\begin{Bmatrix} 0 & k_z & -k_y \\ -k_z & 0 & k_x \\ k_y & -k_x & 0 \end{Bmatrix}\mathbf{F}_0 \tag{24}$$

and

$$\mathbf{H}(x,y) = \mathcal{F}^{-1}\frac{-jc\mathcal{F}u(k_x,k_y)}{k_0} \cdot\begin{Bmatrix} (k_0^2-k_x^2) & -k_xk_y & -k_xk_z \\ -k_xk_y & (k_0^2-k_y^2) & -k_yk_z \\ -k_xk_z & -k_yk_z & (k_0^2-k_z^2) \end{Bmatrix}\mathbf{F}_0 \tag{25}$$

with $k_z = \sqrt{k_0^2-k_x^2-k_y^2}$. Now we can simply calculate $S_\parallel$ via (23) and determine the fraction of the total power that hits the mirror or vacuum window. Of course, we also enforce $u(x,y)=0$ outside the mirror or window surface which leads to side lobes in the emanating beam if there is a significant field at the edges.

4 Iterative Algorithms

In the analysis and synthesis of field distributions in millimeter wave transmission systems we have more degrees of freedom than compared to the "conventional" RF engineering, as the structures are much larger than the wavelength. Although classical methods of non-linear optimization have been successfully applied to oversized components [17], [18], these algorithms are challenged by an increasing number of optimization parameters.

More than half a century ago the basis was formed [19]-[22] for several iterative algorithms which are now commonly used for millimeter wave transmission systems. These algorithms resemble Picard's method for the solution of Fredholm integral equations of the second kind. They rely on the repetitive numerical solution of the diffraction integral, which is why they were somewhat ahead of the times then. When cheap computing power and fast numerical propagators became available these algorithms were refined and brought into practical use mainly by Russian scientists [3], [7], [12], [13], [26], [31], [32], [33]. The idea behind these algorithms is the Picard-like solution of the wave equation by propagating the field back and forth between some input and output. As the solution of the wave equation is not uniqe, the algorithm is "reminded" of the known (analysis) or desired (synthesis) field properties in every iteration. This is also known as error reduction scheme. In view of an optimization we have as many free parameters as there are sampling points with these methods. Therefore the CPU time depending on the number of parameters scales like that of the propagator (the FFT in our case).

There is yet another approach: the method of irradiance moments [23]-[25]. It relies on the fact that the moments of n-th order of the amplitude distribution of a beam can be propagated on the basis of a simple equation. The beam radius of a fundamental gaussian beam corresponds e.g. to the moment of second order. This method has also been successfully applied to high-power microwave components. It is as suitable for the analysis and synthesis of paraxial beams, and it also represents a true synthesis method in contrast to a classical parameter optimization. This method will be compared to the iterative algorithms below.

4.1 Field Analysis

It is relatively simple to measure the amplitude distribution of paraxial millimeter wave beams, whereas it is more difficult to measure the phase distribution. Nevertheless, both entities are required to characterize a beam. Apart from holographic methods which require a known phase-locked reference beam, we can obtain the phase distribution iteratively with an error reduction scheme described in [20],[21],[22]. The algorithm calculates a source phase distribution which produces the known target amplitude distribution together with the known source amplitude distribution:

1. Initialize the source phase distribution with a reasonable guess.
2. Apply the calculated source phase distribution to the measured source amplitude distribution.
3. Propagate the field to the target aperture.

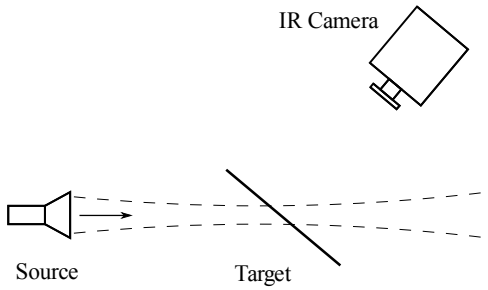

Figure 2: Thermographic Measurement of $|\mathbf{S}|$.

4. End the iteration if the calculated target amplitude distribution is close enough to the measured one.

5. Apply the calculated target phase distribution to the measured target amplitude distribution.

6. Propagate the field back to the source aperture and go back to step 2.

The agreement in step 4 is usually judged by the normalized scalar product of both distributions. A realistic application to millimeter wave beams was first published in [26]. As the solution of the phase retrieval problem is not necessarily unique for two apertures, the authors have extended the above scheme to three (or more) apertures.

The measurement of the amplitude distribution in high-power transmission lines is usually done with infrared images of a thin dielectric target placed in the beam. For the temperature rise of the target we then have $\Delta T \propto |\mathbf{S}| \propto |u|^2$. As the infrared camera has to be placed outside the beam, the image has to be rectified if the target is perpendicular to the optical axis. However, by using (4) we can place the target perpendicular to the camera, see Figure 2. This eliminates the need of an image rectification which is a potential error source.

There are plenty of variations of this phase retrieval algorithm. In case of space constraints it is conceivable to make measurements in different sections of the transmission line with an arbitrary number of (shaped) mirrors in between. It is even possible to leave the target stationary. As a mere revolution of the aperture around an axis other than $\mathbf{e}_z$ provides additional information about the beam, we can reconstruct the phase with a target rotation only, i.e. $d = 0$ in (4). See [27] for an example.

As an application example Figure 3 shows such a reconstructed beam back-propagated to the gyrotron window on the left side and the same beam at the torus window on the right side. There are 7 single-beam mirrors, 7 multi-beam mirrors and two polarizers between both apertures. The total optical path is 58m, see [5] for details. The imaging properties of the transmission line are confirmed by the little side lobe that can be recognized on both pictures.

In [7] the phase reconstruction was applied to the field in a circular corruated waveguide. Here we can make use of the fast cylindrical mode decomposition (10). Another option would be the retrieval the phase of the free space beam from the open ended waveguide and the application of (10) after a backpropagation to the waveguide end.

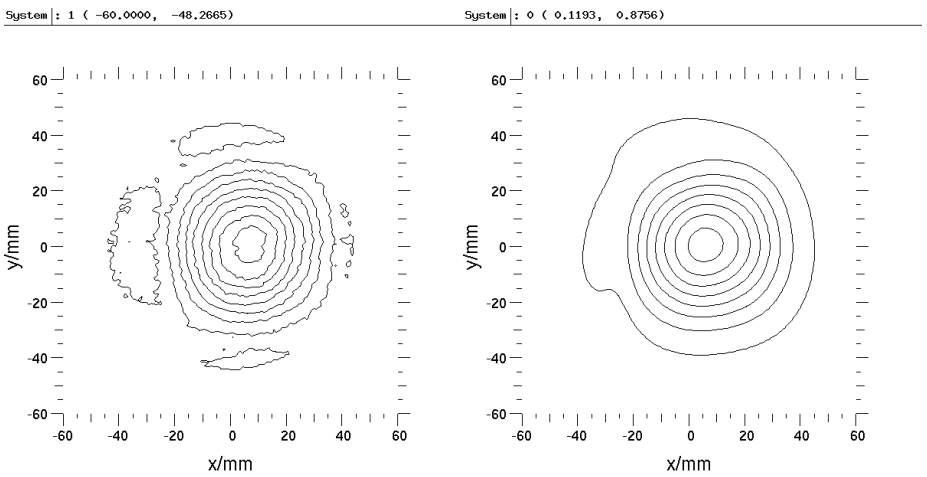

Figure 3: Reconstructed Beam at the Gyrotron Window (left) and at the Torus Window (right)

In [28] a variant of the above algorithm is discussed where the source and target apertures are of cylindrical shape. This is well suited for the phase reconstruction of the output of a helically cut waveguide antenna which transforms the operating mode of the gyrotron into a beam with high divergence in the azimuthal direction and little divergence in the longitudinal direction. Its wavefront has the shape of a spiral with a small slope. Therefore a cylindrical aperture can cover the whole beam with little overhead. Additionally, when measuring the field with a pick-up probe it is important to have the horn always at about the same angle with respect to the wavefront. Due to the directional characteristic of the probe, its signal is generally not proportional to $|u|^2$. A fast spectral domain propagator for this setup is also presented in [28].

A phase reconstruction for plane apertures that are perpendicular to the beam can also be achieved with the method of irradiance moments [24]. It relies on the Fresnel approximation of the diffraction integral, which is justified if the apertures are not too close to each other. The phase distribution of the beam is represented as a low-order polynomial. The unknown polynomial coefficients are obtained by a linear system of equations which is why this is actually not an iterative method. If the phase polynomial is of n^{th} order, $n+1$ measurement planes will be necessary. The main advantage of this method is its resilience against transverse displacements of the different target positions. On the other hand it should be used only if the phase front can be represented with sufficient accuracy with a low order polynomial. This is e.g. not the case for unsymmetric Gauss-Laguerre modes or beams with phase residuals (see below).

4.2 Field Synthesis

The problems of phase retrieval and phase corrector synthesis are equivalent when taking the desired target amplitude distribution instead of the distribution which results from the given phase at the source. If there is a physical solution, the above algorithm will find a source phase distribution which produces the

desired target amplitude pattern, e.g. it should not violate Liouville's theorem. In case of a non-physical desired target amplitude, the achieved pattern will be only close to the desired one. The difference between the synthesized and the given source phase distribution is compensated by a phase corrector. The difference between the achieved and the desired target phase distribution is compensated by a second phase corrector. This results in a pair of matching mirrors or lenses for paraxial beams [3].

In order to produce a lens or a mirror, a phase corrector has to be translated into a height modulation according to section 3.2. This height modulation has to be smooth to keep the stray radiation level low. For the phase corrector $\varphi(x, y)$ the task is to find a function $\psi(x, y) = \varphi(x, y) + 2\pi n(x, y)$ where n is an integer and $|\nabla\psi|$ is always finite. We call this procedure *unwrapping*. This two-dimensional problem is generally not solvable for numerically given phase distributions or unsymmetric Gauss-Laguerre beams. There usually remain residual points which are similar to screw displacements in crystals. The one-dimensional unwrapping along a closed path around the residual point results in a step of $n2\pi$ at the start/end point. Although this is not a step in the phase distribution, it represents an undesired step in the height modulation. There are many path-dependent and pathless algorithms to treat this problem, see e.g. [29].

Now the actual task is to produce a smooth height modulation with a low phase error at positions where the amplitude is high. A proven method which follows this principle is discussed in [28]. The synthesized smooth mirrors will generally produce a field which is only close to that of the ideal phase correctors. If the result is not satisfactory it is possible to place two (or more) "auxiliary" phase correctors recursively inbetween the original source and target [30].

For mirrors that change the wavefront significanly, it is possible to apply the synthesis algorithm to deep mirrors as described in section 3.2. Here we use a predefined deep but smooth mirror as an initial guess. During the synthesis we use only the valid points in each slice for the replacement of the amplitude distribution. For the unwrapping the phase distribution is flattened by substracting the phase shift that corresponds to the initial guess. Then the resulting phase corrector is just a tiny perturbation on top of the initial guess. Note that the problem of cross-polarization generally arises for such mirrors.

The method of irradiance moments is also suitable for the synthesis of mirrors [25]. The second phase corrector of a mirror pair is a 2D polynomial of low order. This has the inherent advantage that the mirror is smooth and has no residual points, i.e. it needs no unwrapping. The coefficients of the polynomial are the solution of a nonlinear system of equations. Again, this is actually not an iterative method, although the equations are finally solved with the Newton method. The target distribution must be Gaussian to provide analytic expressions for the backpropagated moments. These are rather large expressions which can nevertheless be handled by a computer algebra system. Like the field analysis, this method relies on the Fresnel approximation of the diffraction integral. Depending on the order of the polynomial and the incoming wavefront, the first mirror will also be smooth but it needs unwrapping and can have residual points.

A waveguide wall can also be regarded as a recursive mirror. This approach leads to methods for the shaping of the waveguide wall in such a way that a desired field can be synthesized at the wave guide end [12], [13]. These methods

are basically variations of the error reduction scheme as described above. The difference between the forward propagated given field and the backward propagated desired field becomes smaller in each iteration through a perturbation of waveguide wall according to their phase difference. Finally the forward and backward propagated fields will converge. This phase corrector approach is applicable as long as the mode spectrum is narrow. This is the same assumption as for the shallow mirrors in section 3.2.

Another concept that follows the error reduction scheme decomposes the given and the desired field into cylindrical modes which are coupled due to wall perturbations [31], [32]. The coupled modes are described by a system of ordinary linear differential equations that can be solved forward for the given field at the waveguide input and backward for the desired field at the waveguide output. The coupling coefficients for the modes and hence the wall perturbations are modified in each longitudinal position so that the difference between the backward and forward field becomes smaller in every iteration. However, the wall perturbations must be small enough to ensure the validity of the coupled mode equations.

The above methods usually reduce the error reduction algorithm to a scalar problem like (3). This is not the case for the most general variant of this scheme which is proposed in [33]. It relies on the forward and backward solution of the field by a general purpose electromagnetics code. With the advent of fast multipole techniques and more powerful computing clusters this method has a high potential for a broad variety of synthesis problems despite the requirement of larger computing ressources. The applications range from overmoded waveguides to deep mirrors. Depending on the electromagnetic solver, this method does not rely on approximations concerning the validity of the field solution. Therefore large deformations can also be synthesized and cross polarization can be a concern. However, convergence is not guaranteed, and the magnitude and spatial filtering of the conducting walls in each iteration have to be carefully adjusted.

5 Conclusion

A framework for the numerical calculation of high power millimeter wave transmission lines has been discussed. It permits the treatment of larger systems with a feasible numerical effort while still preserving the complete field quantities. This can be useful for the characterization and design of transmission lines, as well as for the delivery of a real-world input to full-wave plasma physics codes.

A brief overview over iterative algorithms was provided for which fast propagators are essential. The phase reconstruction and synthesis methods have become state of the art, and have proven their practical applicability. Due to the large number of free parameters, the direct synthesis has turned out to be more than competitive to the classical approach of non-linear optimization.

The design of broadband components—which is beyond the scope of this article—is currently a very active field. Most of the above synthesis algorithms have been extended to broadband variants, and the develpoment is still ongoing. Due to the computational efficiency of the propagators, the analysis for a number of frequencies is still a feasible task.

A very recent field are resonant beam switches and combiners. Their behav-

ior is controlled additionally by the input frequency which offers a wide range of applications, see [34] for details. Due to their resonant behavior, we no longer have just a forward propagation in the analysis. Nevertheless, such components can be integrated in the overall model via Fox-Li iterations or self-consistent EM solvers by means of the given interface techniques.

References

[1] M. Thumm and W. Kasparek, "Passive High-Power Microwave Components", *IEEE Trans. Plasma Sci.*, vol. 30, pp. 755-786, June 2002.

[2] G. Michel and M. Thumm, "Spectral Domain Techniques for Field Pattern Analysis and Synthesis", *Surv. Math. Ind.*, vol. 8, pp. 259-270, 1999

[3] A.A. Bogdashov, A.B. Chirkov, G.G. Denisov, D.V. Vinogradov, A.N. Kuftin, V.I. Malygin, V.E. Zapevalov, "Mirror Synthesis for Gyrotron Quasi-Optical Mode Converters", Int. J. of IRMM Waves, vol. 16, pp. 735ff, 1995

[4] R.N. Bracewell, "The Fourier Transform and Its Applications", McGraw-Hill, New York, 1965

[5] G. Michel and W. Kasparek, "Numerical Analysis of the W7-X ECRH Transmission Line", in A.G. Litvak (Ed.), *Strong Microwaves: Sources and Applications*, vol. 2, pp. 337ff, IAP RAS, Nizhny Novgorod, 2009

[6] P.-S. Kildal, "Artificially Soft and Hard Surfaces in Electromagnetics", *IEEE Trans. Ant. Prop.*, vol. 38, No. 10, pp. 1537ff, 1990

[7] N.L. Aleksandrov, A.V. Chirkov, G.G Denisov, S.V. Kuzikov, "Mode Content Analysis from Intensity Measurements in a Few Cross Sections of Oversized Waveguides", *Int. J. of IRMM Waves*, vol. 18, No. 6, pp. 1323ff, 1997

[8] J.L. Doane, "Propagation and Mode Coupling in Corrugated and Smooth-Wall Circular Waveguides", *Infrared and Millimeter Waves*, vol. 13, pp. 123ff, 1985

[9] C.P. Moeller, "A method of remotely steering a microwave beam launcher from a highly overmoded corrugated waveguide", *Proc. 23rd Conf. IRMMW*, pp. 116ff, 1998

[10] S.V. Kuzikov, "Wave beam multiplication phenomena to RF power distribution systems of high-energy linear accelerators", *Int. J. of IRMM Waves*, vol. 19, pp. 1523ff, 1998

[11] A.A. Bogdashov, G.G. Denisov, "Asymptotic Theory of High-Efficiency Converters of Higher-Order Waveguide Modes Into Eigenwaves of Open Mirror Lines", *Radiophys. Quantum Electr.*, vol. 47, No.4, pp. 283ff, 2004

[12] S.V. Kuzikov, "Paraxial Approach to Description of Wave Propagation in Irregular Oversized Waveguides", *Int. J. of IRMM Waves*, vol. 18, No. 5, pp. 1001ff, 1997

[13] A.V. Chirkov, G.G. Densiov, M.L. Kulygin, V.I. Malygin, S.A. Malygin, A.B. Pavel'ev, E.A. Soluyanova, "Use of Huygens' Principle for Analysis and Synthesis of the Field in Oversized Waveguides", *Radiophys. Quantum Electr.*, vol. 49, No. 5, pp. 344ff, 2006

[14] J. Neilson, "Electric Field Integral Equation Analysis and Advanced Optimization of Quasi-Optical Launchers used in High Power Gyrotrons,", *NATO Science Series II: Mathematics, Physics and Chemistry, Quasi-Optical Control of Intense Microwave Transmission*, Vol. 203, July 2005

[15] G. Michel, O. Prinz, T. Rzesnicki, "Mode converter design for coaxial gyrotrons", *Proc. 30th Conf. IRMM Waves*, vol. 2, pp. 373ff, 2005

[16] D. Wagner, F. Leuterer, "Broadband Polarizers for High-Power Multi-Frequency ECRH Systems", *Int. J. of IRMM Waves*, vol. 26, No. 2, pp. 163ff, 2005

[17] B. Plaum, D. Wagner, W. Kasparek, M. Thumm, "Optimization of Oversized Waveguide Components Using a Genetic Algorithm", *Fusion Eng. Design*, vol. 53, pp. 499ff, 2001

[18] J. M. Neilson, "Optimal Synthesis of Quasi-Optical Launchers for High-Power Gyrotrons", *IEEE Trans. Plasma Sci.*, vol. 34, No. 3, pp. 635ff, 2006

[19] L.B. Tartakovsky, "Synthesis of a Linear Radiator and its Analogy to the Problem of Broadband Matching" (in Russian), *Radiotekhnika i Elektronika*, vol. 12, pp. 1463ff, 1958

[20] L.B. Tartakovsky, W.K. Tikhonova, "Synthesis of a Linear Radiator with a Known Amplitude Distribution" (in Russian), *Radiotekhnika i Elektronika*, vol. 12, pp. 2016ff, 1959

[21] B.Z. Katzenelenbaum, V.V. Semenov, "Synthesis of Phase Correctors Shaping a Specified Field", *Radio Eng. Electron. Phys.*, vol. 12, pp. 233ff, 1967

[22] R.W. Gerchberg, W.O. Saxton, "A Practical Algorithm for the Determination of Phase from Image and Diffraction Plane Pictures", *Optik*, vol. 35, pp. 237ff, 1972

[23] M.R. Teague, "Irradiance Moments: Their propagation and Use for Unique Phase Retrieval", *J. Opt. Soc. Amer.*, vol. 72, No. 9, pp. 1199ff, 1982

[24] J.P. Anderson, M.A. Shapiro, R.J. Temkin, D.R. Denison, "Phase retrieval of Gyrotron Beams Based on Irradiance Moments", *IEEE Trans. MTT*, vol. 50, No. 6, pp. 1526ff, 2002

[25] M.A. Shapiro, J.P. Anderson, R.J. Temkin, "Synthesis of Gyrotron Phase Correcting Mirrors Using Irradiance Moments", *IEEE Trans. MTT*, vol. 53, No. 8, pp. 2610ff, 2005

[26] A.V. Chirkov, G.G. Denisov, N.L. Aleksandrov, "3D Wavebeam Field Reconstruction from Intensity Measurements in a Few Cross Sections", Opt. Comm., vol. 115, pp. 449ff, 1995

[27] G. Michel, "Another variant of the Katzenelenbaum-Semenov Algorithm", *Proc. 28th Conf. IRMM Waves*, pp. 263ff, 2003

[28] M.P. Perkins, R.J. Vernon, "Mirror Design for Use in Gyrotron Quasi-Optical Mode Converters", *IEEE Trans. Plasma Sci.*, vol. 35, No. 6, pp. 1747ff, 2007

[29] D.C. Ghiglia, M.D. Pritt, "Two-dimensional Phase Unwrapping: Theory, Algorithms and Software", Wiley, New York, 1998

[30] Y. Hirata, Y. Mitsunaka, K. Hayashi, Y. Itoh, "Wave-Beam Shaping Using Multiple Phase-Correction Mirrors", *IEEE Trans. MTT*, vol. 45, No. 1, pp. 72ff, 1997

[31] G.G. Denisov, G.I. Kalynova, D.I. Sobolev, "Method for Synthesis of Waveguide Mode Converters", *Radiophys. Quantum Electr.*, vol. 47, No. 8, pp.615ff, 2004

[32] G.G. Denisov, S.V. Samsonov, D.I. Sobolev, "Two-Dimensional Realization of a Method for Synthesis of Waveguide Converters", *Radiophys. Quantum Electr.*, vol. 49, No. 12, pp.961ff, 2006

[33] S.V. Kuzikov, M.E. Plotkin, "Synthesis of Mode Converters for High-Power Microwave Sources", in A.G. Litvak (Ed.), *Strong Microwaves: Sources and Applications*, vol. 1, pp. 201ff, IAP RAS, Nizhny Novgorod, 2009

[34] A. Bruschi, V. Erckmann, W. Kasparek, M. Petelin et. al., "Diplexers for Power Combination and Switching in High-Power ECRH Systems", *this issue*

Georg Michel was born in Karl-Marx-Stadt, former East-Germany, in 1964. He received the Dipl.-Ing. degree from Technische Universität Ilmenau, Germany, in 1994 and the Dr.-Ing. degree from Universität Karlsruhe (TH), Germany, in 1998.

Since 1999 he has been with the Max-Planck-Institut für Plasmaphysik, TI Greifswald, Germany. His research interests focus on programmable logic and embedded computing as well as numerical simulation of electromagnetic fields.